THE JOURNAL OF BIOLOGICAL CHEMISTRY VOL. 287, NO. 24, pp. 20395–20406, June 8, 2012

Asymmetry in the Homodimeric ABC Transporter MsbA Recognized by a DARPin*[S]

Received for publication, March 7, 2012, and in revised form, April 2, 2012 Published, JBC Papers in Press, April 20, 2012, DOI 10.1074/jbc.M112.359794

Anshumali Mittal[‡1], **Simon Böhm**[§], **Markus G. Grütter**[‡], **Enrica Bordignon**[§2], **and Markus A. Seeger**[‡3]

From the [‡]*Department of Biochemistry, University of Zurich, 8057 Zurich, Switzerland and the* [§]*Laboratory of Physical Chemistry, ETH Zurich, 8093 Zurich, Switzerland*

Background: ABC exporters are suggested to hydrolyze ATP sequentially implying the existence of asymmetries.
Results: An *in vitro* selected binder (DARPin) was identified that binds to homodimeric MsbA at a stoichiometric ratio of 1:1.
Conclusion: The DARPin recognizes asymmetries in MsbA.
Significance: Selected binding proteins are useful tools to recognize membrane transporters in novel conformational states.

ABC transporters harness the energy from ATP binding and hydrolysis to translocate substrates across the membrane. Binding of two ATP molecules at the nucleotide binding domains (NBDs) leads to the formation of an outward-facing state. The conformational changes required to reset the transporter to the inward-facing state are initiated by sequential hydrolysis of the bound nucleotides. In a homodimeric ABC exporter such as MsbA responsible for lipid A transport in *Escherichia coli*, sequential ATP hydrolysis implies the existence of an asymmetric conformation. Here we report the *in vitro* selection of a designed ankyrin repeat protein (DARPin) specifically binding to detergent-solubilized MsbA. Only one DARPin binds to the homodimeric transporter in the absence as well as in the presence of nucleotides, suggesting that it recognizes asymmetries in MsbA. DARPin binding increases the rate of ATP hydrolysis by a factor of two independent of the substrate-induced ATPase stimulation. Electron paramagnetic resonance (EPR) measurements are found to be in good agreement with the available crystal structures and reveal that DARPin binding does not affect the large nucleotide-driven conformational changes of MsbA. The binding epitope was mapped by cross-linking and EPR to the membrane-spanning part of the transmembrane domain (TMD). Using cross-linked DARPin-MsbA complexes, 8-azido-ATP was found to preferentially photolabel one chain of the homodimer, suggesting that the asymmetries captured by DARPin binding at the TMDs are propagated to the NBDs. This work demonstrates that *in vitro* selected binders are useful tools to study the mechanism of membrane proteins.

ATP-binding cassette (ABC)[4] transporters are primary active transporters, which act as exporters, importers, receptors, and channels. These transmembrane proteins mediate a plethora of physiological phenomena, including transport of metabolic products, nutrients, proteins, peptides, lipids, polysaccharides, ions, and drugs (1). In humans, malfunction of ABC transporters leads to several genetic disorders including cystic fibrosis, neurological diseases, retinal degeneration, cholesterol, and bile transport defects, anemia, and insufficient drug response.

MsbA is a homodimeric ABC exporter involved in the transport of lipid A and lipopolysaccharides to the outer leaflet of the inner membrane of several Gram-negative bacteria (2), and the *msbA* gene is essential in *Escherichia coli* (3). MsbA is homologous to the multidrug transporter LmrA of Gram-positive *Lactococcus lactis* (4) and mammalian multidrug resistance transporters such as P-glycoprotein (5) and shows overlapping substrate specificity with them (6, 7). At a molecular level, ABC transporters consist of four domains, two transmembrane domains (TMDs) and two nucleotide-binding domains (NBDs). In ABC exporters, the TMDs are composed of at least six transmembrane helices, which form the substrate transport pathway and provide specificity. The NBDs are also known as ATP-binding cassettes and drive the transport cycle by binding and hydrolyzing ATP. The motional energy of the NBDs are coupled to conformational changes in the TMDs which alternate between an inward- and an outward-facing state and thereby form a pathway to mediate unidirectional transport across the membrane (8).

Current molecular understanding of ABC exporters is based on crystal structures of Sav1866 (8) solved at 3 Å in its outward-facing state, P-glycoprotein solved at 3.8 Å in its inward-facing state (5), and the structures of three homologues of MsbA solved in three different conformations at resolutions ranging

* This work was funded by the Swiss NCCR Structural Biology program, an Ambizione Grant from the Swiss National Science Foundation (to M. A. S.) and a Forschungskredit of the University of Zurich (to M. A. S.).
[S] This article contains supplemental Figs. S1–S10 and Table S1.
[1] Affiliated with the Ph.D. Program in Molecular Life Sciences of the Life Science Zurich Graduate School.
[2] To whom correspondence may be addressed: Laboratory of Physical Chemistry, ETH Zurich, Switzerland; E-mail: enrica.bordignon@phys.chem.ethz.ch.
[3] To whom correspondence may be addressed: Department of Biochemistry, University of Zurich, Switzerland; E-mail: m.seeger@bioc.uzh.ch.

[4] The abbreviations used are: ABC, ATP-binding cassette; DARPins, designed ankyrin repeat proteins; EPR, electron paramagnetic resonance; ISOVs, inside-out vesicles; RSOVs, right-side-out vesicles; SEC, size exclusion chromatography; DEER, Double Electron Electron Resonance; AMP-PNP, adenosine 5′-(β,γ-imino)triphosphate; TMD, transmembrane domain; NBD, nucleotide binding domain, M5M, 1,5-pentanediyl bismethanethiosulfonate; M11M, 3,6,9-trioxaundecane-1,11-diyl-bismethanethiosulfonate; DTT, dithiothreitol; MTSSL, 1-oxyl-2,2,5,5-tetramethyl-Δ3-pyrroline-3-methyl) methanethiosulfonate.

from 3.7 Å to 5.5 Å (9). Based on these crystal structures, large conformational changes are expected to occur in ABC exporters upon nucleotide binding and hydrolysis, which could be confirmed by cross-linking experiments and EPR measurements (10–14).

The mechanistic details of how the binding and hydrolysis of ATP at the NBDs is coupled to the transport process at the TMDs are still a matter of controversy. In many heterodimeric ABC transporters, one of the two ATPase sites deviates from the consensus sequence and is therefore called the degenerate site (15). Such heterodimeric ABC exporters mainly hydrolyze ATP at the consensus site and thus operate in an asymmetric fashion. In homodimeric ABC exporters such as BmrA as well as in P-glycoprotein which is a fused heterodimer but exhibits two consensus ATPase sites, biochemical experiments demonstrated that only one ATP molecule is trapped by vanadate in the post-hydrolytic state per ABC transporter dimer (16, 17). It was concluded that ABC exporters hydrolyze the two ATP molecules sequentially instead of simultaneously, possibly involving a mechanism of alternating catalytic sites (18). This mechanism implies that the NBD homodimer must switch to an asymmetric conformation before ATP is hydrolyzed at one of the two catalytic sites. In support of this notion, asymmetric homodimers have been observed in crystal structures of the ATP-bound NBDs of the ABC transporter HlyB (19). On the other hand, current crystal structures of outward-facing MsbA and Sav1866 feature two bound AMP-PNP at the NBDs (thus representing a pre-hydrolytic state) and display only minor structural differences between the two chains, that are related by 2-fold non-crystallographic symmetry (9, 20). Molecular dynamics simulation using the symmetric Sav1866 and MsbA structures as starting points revealed that the NBDs readily switch to an asymmetric state in which only one molecule of ATP enters the hydrolysis reaction at a time (21, 22). Further work addressing the question of asymmetry in ABC exporters is clearly needed to resolve the apparent discrepancies between asymmetries found based on biochemical experiments and the symmetric crystal structures of the homodimers Sav1866 and MsbA.

Designed Ankyrin Repeat Proteins (DARPins) represent a well-established randomized scaffold used as an alternative to antibody fragments (Fabs and scFvs) and have been selected against a variety of target proteins (23–25). A growing number of DARPin co-crystal structures demonstrate the successful application of such designed binding proteins as crystallization aids (24). Besides possible improvements of crystal diffraction, DARPins have the potential to trap the targeted protein in alternate conformations. DARPins selected against the multidrug transporter AcrB for example trap this protein in an asymmetric state with two DARPins bound to the homotrimer (25, 26). In the absence of DARPins, AcrB was initially crystallized in its symmetric and later in its asymmetric state (27, 28).

Here, we describe the selection of DARPins against detergent-purified MsbA using ribosome display. We identified a DARPin which binds to the homodimeric transporter in a 1:1 stoichiometric ratio. The DARPin binding epitope was mapped to the TMDs and was found to be located away from the 2-fold symmetry axis of MsbA, suggesting that the DARPin recognizes asymmetries in MsbA. DEER measurements revealed that addition of the DARPin to MsbA does not influence the large ATP-induced conformational changes during transporter cycling. Nevertheless, DARPin binding enhances the basal ATPase activity of the transporter without impairing the substrate-induced stimulation suggesting that the catalytic cycle is accelerated when asymmetric MsbA conformations are populated.

EXPERIMENTAL PROCEDURES

Purification, Biotinylation, and Spin Labeling of MsbA and DARPin—A detailed description of the cloning, expression, and purification of MsbA is given in the supplemental Experimental Procedures. MsbA was expressed in *E. coli* C43 (DE3) cells from a pBAD vector and purified using β-UDM as detergent. DARPin expression and purification has been described previously (29). Enzymatic biotinylation was facilitated by fusing an Avi-tag sequence to the of MsbA. Single cysteine mutants at positions A25C, R103C, N191C, S206C, and S246C of MsbA were introduced by site-directed mutagenesis taking Cys-less *msbA* (C88S/C315S) as template. Likewise, single cysteine mutants were also introduced into the N- and C-terminal caps of DARPin_55 (which is Cys-less by design) at the positions S12C, K16C, E29C, D151C, and D160C. For methanethiosulfonate cross-linking and spin labeling, single cysteine mutants of MsbA and DARPin were purified by supplementing 5 mM dithiothreitol (DTT), which was removed (PD-10 column, GE Healthcare) prior to labeling with 10 times molar excess of MTSSL ((1-oxyl-2,2,5,5-tetramethyl-Δ3-pyrroline-3-methyl) methanethiosulfonate; Toronto Research Chemicals). Excess spin label was removed by size exclusion chromatography. For the EPR measurements, DARPin-MsbA complexes were made by spin labeling the freshly purified proteins individually, followed by gel-filtration of the protein complex.

Selection and Screening of DARPin Specific to MsbA—The N3C DARPin library (23) was used for binder selection by ribosome display as described (25, 30). Four rounds of selections were carried out following the solution panning strategy (29). 0.05% of β-UDM were used to maintain MsbA in active form. Single clones of the enriched pool of DARPins from the 4th selection round were expressed from the vector $pQE30_{myc5}$ (29)in *E. coli* XL-1 Blue yielding DARPins carrying an N-terminal RGS-His_6 tag (MRGSHHHHHH) and a C-terminal Myc_5 tag (5 times amino acid sequence MEQKLISEEDLNE). Single DARPin clones were analyzed for binding to $bMsbA_{AviC}$ by crude cell extract ELISAs as described previously (29).

SEC of Isolated DARPins and the MsbA-DARPin Complexes—ELISA-positive MsbA-specific DARPins were subcloned into pQE30 (Qiagen) devoid of the C-terminal Myc_5 tag for further biochemical analysis. A molar excess (2 to 3 times) of freshly gel-filtrated monomeric DARPins were mixed with MsbA and incubated in 20 mM Tris/HCl (pH 7.5), 150 mM NaCl, and 0.05% β-UDM for at least 30 min at 4 °C for complex formation. The protein complex was separated on a Superdex 200 10/300 GL column (GE Healthcare) (supplemental Fig. S4). The fractions corresponding to the MsbA-DARPin complex were analyzed by on-chip protein analysis according to the manufacturer's protocol (Protein 80 Kit, Agilent Technologies) (supplemental Fig. S8).

Cysteine Cross-linking of MsbA and DARPin_55 Mutants—For cross-linking studies, two thiol-specific homobifunctional cross-linkers namely M5M (1,5-pentanediyl bismethanethiosulfonate, Toronto Research Chemicals) and M11M (3,6,9-trioxaundecane-1,11-diyl-bismethanethiosulfonate, Toronto Research Chemicals) with spacer arms of 9.1 Å and 16.9 Å were used (32). The MsbA and DARPin_55 mutant proteins were mixed at ratios of 1:3 and incubated with 0.5 mM of cross-linker for 15 min at 4 °C (if not stated otherwise). The reactions were stopped by addition of SDS sample buffer and separated by non-reducing SDS-PAGE. The ability of DARPin_55_29C to cross-link to MsbA_191C was also tested using inside-out membrane vesicles (ISOVs) containing overexpressed MsbA_191C (with detergent purified MsbA_191C, this cross-link is readily formed). To this end, MsbA_191C containing ISOVs (6 mg in 3 ml) were mixed with DARPin_55_29C (35 mg in 7 ml) and M11M (1 mM) was added. After incubation for 30 min, *N*-ethylmaleimide (NEM, 10 mM) was added to react with the remaining free cysteines for another 30 min. Subsequently, MsbA was purified according to the standard protocol and subjected to non-reducing SDS-PAGE (supplemental Fig. S8).

ATPase Assay—The ATPase activity of purified protein was measured from the release of P_i from ATP in a colorimetric malachite green assay as described (33). Briefly, purified protein (200 nM) in 50 mM K-HEPES buffer pH 7.4 containing 0.05% β-UMD, 2.5 mM $MgCl_2$ and 2 mM ATP was incubated at 30 °C in a total reaction volume of 50 μl for 10–15 min. MsbA was inactivated by heating at 80 °C for 2 min and free P_i was measured using malachite green solution. The A_{600} of the samples was measured in a Microplate reader Infinite M100 (TECAN) and compared with the A_{600} of standards containing 0.5–4 nmol P_i. Readings were corrected for P_i contamination originating from the ATP and buffer. DARPin_55-stimulated ATPase activity of MsbA was performed by adding DARPin_55 at concentrations as indicated to MsbA (200 nM) 15 min prior to the assay start. All cysteine mutants used in this study showed ATPase activity comparable to the wild-type. Spin labeling did not affect the activity of MsbA (supplemental Table S1).

Reconstitution of MsbA into Liposomes—Detergent-purified MsbA was reconstituted into lipid membrane vesicles made of polar *E. coli* lipids and egg phosphatidylcholine mixed at a ratio of 3:1 (34). For EPR and DARPin binding experiments, the reconstitution buffer was 20 mM Tris/HCl pH 7.4, 150 mM NaCl, for ATPase activity measurements it was 50 mM K-HEPES pH 7.0. $MgCl_2$ was added only where indicated shortly before performing ATPase activity or EPR experiments to avoid aggregation of the liposomes. The amount of reconstituted MsbA was determined by the Bio-Rad D_C Protein Assay according to manufacturer's protocol and compared BSA protein concentration standards. Binding of DARPin_55 to the reconstituted MsbA was tested by incubating the DARPin_55 with reconstituted MsbA (3:1 ratios) or empty liposomes for 15 min at 4 °C. Unbound DARPin_55 was removed by three buffer washes after centrifugation at 20,000 × *g* for 20 min at 4 °C. The pelleted liposomes were dissolved in SDS buffer and were separated by SDS-PAGE (15% acrylamide gel) followed by SYPRO ruby staining (supplemental Fig. S6*B*).

Distance Measurements by Pulse EPR Experiments—Dipolar time evolution data were acquired using the four-pulse DEER (Double Electron Electron Resonance) experiment (35). DEER traces were measured in a home-made high power Q band spectrometer equipped with a home-made oversized resonator (36). All pulse lengths were set to 12 ns and deuterium modulation artifacts were averaged (8 times d1 time increment of 16 ns). The pump frequency was placed at the maximum intensity of the nitroxide spectrum, and the observer frequency 80 MHz lower. All samples were prepared independently from different batches and the DEER traces were found to be reproducible. Samples contained 10% (*v*/*v*) d8-glycerol and were shock-frozen in liquid nitrogen before measurement. Data analysis was performed with the software DeerAnalysis 2010 (37). The simulation of the possible spin label rotamers attached at selected positions in MsbA was performed using the Matlab program package MMM based on a rotamer library approach (38).

8-N_3-[α-^{32}P]ATP Photolabeling—MsbA191C (1.5 μM) and DARPin_55_29C (6 μM) were cross-linked with M11M (1.5 mM) in 20 mM Tris, pH 7.5, 150 mM NaCl, 0.05% β-UDM containing 3 mM $MgCl_2$. 8-N_3-[α-^{32}P]ATP (1 μM, 0.6 Ci/mmol) was added to 10 μl protein sample (quadruplicates), and the reaction mixtures were incubated at 25 °C for 5 min followed by UV irradiation (100 millijoules, UV cross-linker, Hoefer) on ice. Labeled cross-linked MsbA-DARPin complex was analyzed by SDS-PAGE and photolabeling was quantified using a phosphor imager (Molecular Dynamics, Storm 840). To analyze the amount of cross-linking, four aliquots were supplemented with cold 8-N_3-ATP followed by UV radiation, SDS-PAGE and staining with SYPRO Ruby (Invitrogen). The fluorescent signal was read with the LAS-3000 imaging system, and the bands were quantified using the Aida software (Raytest).

RESULTS

In Vitro Selection and Identification of DARPins Specific for MsbA—DARPin selection against biotinylated avi-tagged MsbA ($bMsbA_{AviC}$) was performed using ribosome display with a DARPin library containing three randomized modules (23, 31, 39) (supplemental Fig. S1). From 2000 DARPin clones analyzed for binding to $bMsbA_{AviC}$ by an initial ELISA (supplemental Fig. S2), 42 DARPins were further analyzed using a specificity ELISA in which besides $bMsbA_{AviC}$ the ABC transporter LmrCD and the secondary-active multidrug transporter AcrB (both prepared as biotinylated Avi-tagged proteins) were used (supplemental Fig. S3). This assay revealed 37 MsbA-specific DARPins that were further analyzed by size-exclusion chromatography. 27 of these DARPins displayed various degrees of oligomerization (soluble aggregates) and 6 of them showed monomer/dimer equilibrium and were therefore excluded. The remaining 4 MsbA-specific DARPins were monomeric but only one DARPin (named DARPin_55) formed a stable complex with MsbA that could be isolated by size exclusion chromatography (supplemental Fig. S4). The affinity of DARPin_55 for MsbA was estimated by competition ELISA (23), in which the binding of $bMsbA_{AviC}$ to immobilized $DARPin\_55_{myc5}$ was competed by pre-incubation with increasing amounts of free DARPin_55. The dissociation constant K_D derived from these experiments was 80 nM (supplemental Fig. S5). Hence, from

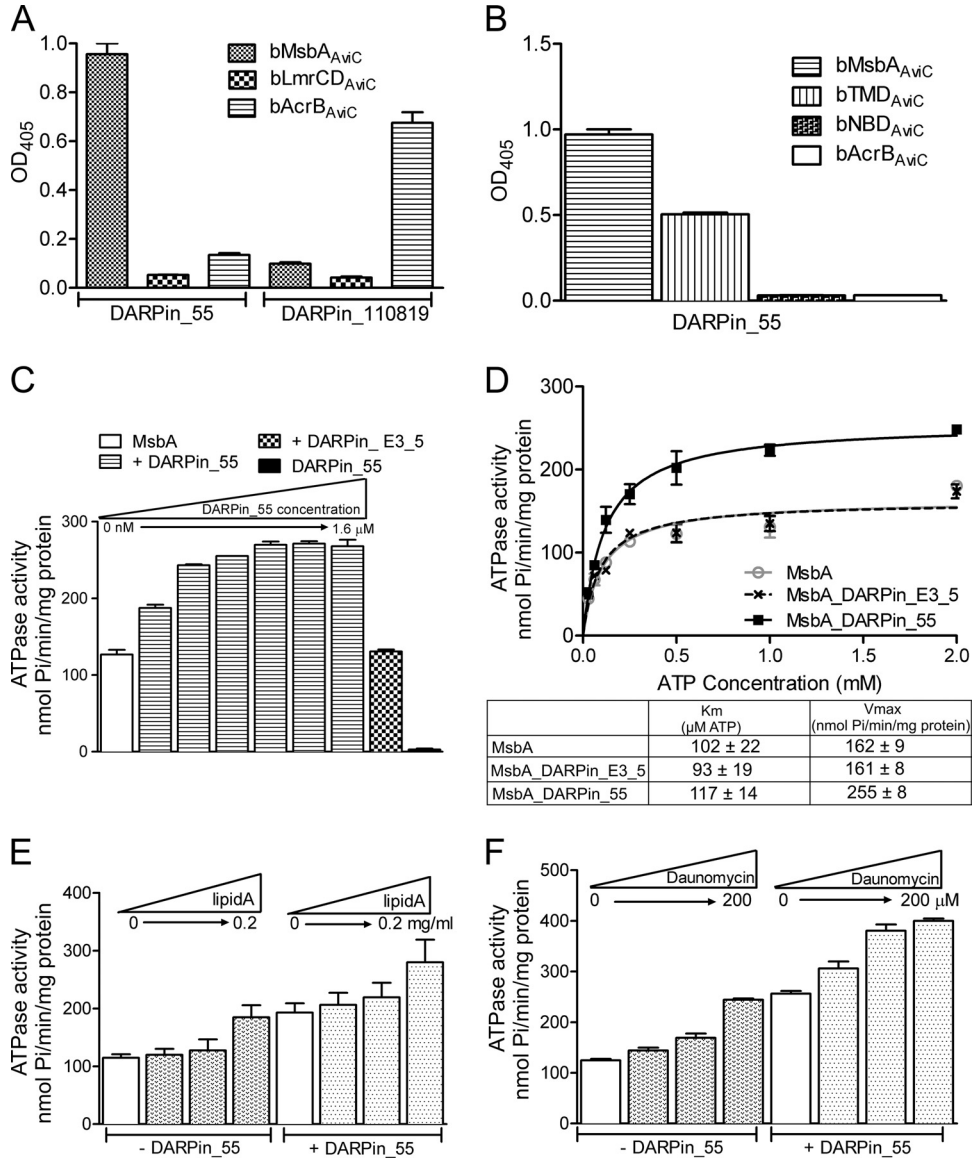

	Km (μM ATP)	Vmax (nmol Pi/min/mg protein)
MsbA	102 ± 22	162 ± 9
MsbA_DARPin_E3_5	93 ± 19	161 ± 8
MsbA_DARPin_55	117 ± 14	255 ± 8

FIGURE 1. **Characterization of DARPin_55: Specificity, epitope mapping and modulation of ATPase activity of MsbA.** *A*, ELISA to determine binding specificity of DARPin_55. DARPin_55 specifically binds to its target protein bMsbA$_{AviC}$ but not to the control proteins bLmrCD$_{AviC}$ and bAcrB$_{AviC}$. DARPin_110819 specifically recognizing bAcrB$_{AviC}$ was used as a control. *B*, ELISA assay to delineate DARPin_55 binding to subdomains of MsbA. DARPin_55 binds to the transmembrane domain (bTMD$_{AviC}$) but not to the nucleotide binding domain (bNBD$_{AviC}$) of MsbA. bAcrB$_{AviC}$ is used as a negative control. *C*, modulation of basal ATPase activity of detergent-solubilized MsbA in complex with DARPin_55. DARPin_55 was added to MsbA (200 nM) in a 2-fold serial dilution series ranging from 50 nM to 1.6 μM leading to a stimulation of the ATPase activity of MsbA by up to 2.1-fold. Addition of the unselected DARPin E3_5 (1 μM) to MsbA does not increase its ATPase activity. DARPin_55 (1 μM) alone does not hydrolyze ATP. *D*, ATPase activity of MsbA was determined in the presence of DARPin_55 (1 μM) or E3_5 (1 μM) as well as in absence of DARPins at varying ATP concentrations. Addition of DARPin_55 results in a higher maximal rate of ATP hydrolysis (V_{max}), while the apparent affinity for ATP (K_m) is not affected. *E* and *F*, stimulations of the ATPase activity of MsbA by substrates and DARPin_55 are additive. Lipid A was added to detergent-purified MsbA at concentrations of 0, 0.05, 0.1, and 0.2 mg/ml *E*, daunomycin was added at concentrations of 0, 50, 100, and 200 μM *F* and ATPase was measured in the absence and presence of DARPin_55 (1 μM). Error bars represent standard deviations.

2000 potential DARPin binders analyzed, we could identify one specific high-affinity binder (Fig. 1*A*).

The ATPase Activity of MsbA Is Stimulated upon Complex Formation with DARPin_55—The effect of DARPin binding to MsbA was studied with respect to the ATPase activity of the transporter. The basal ATPase activity of detergent-purified MsbA (200 nM) was stimulated up to 2.1-fold upon complex formation with DARPin_55 (serial dilution from 50 nM to 1.6 μM) in a dose-dependent manner reaching its maximum at a concentration of 400 nM DARPin_55 (Fig. 1*C*). Addition of the control DARPin E3_5 (39, 40) did not alter the ATPase activity of MsbA and DARPin_55 alone did not hydrolyze ATP. By determining the Michaelis-Menten kinetics of ATP hydrolysis it was found that DARPin_55 binding increases the maximal velocity V_{max} (increase from 162 ± 9 to 255 ± 8 nmol P_i/min/mg MsbA) while the apparent K_m of the ATPase activity remains unchanged (102 ± 22 and 117 ± 14 μM ATP for MsbA and the MsbA/DARPin_55 complex, respectively) (Fig. 1*D*). Lipid A and daunomycin are known substrates of MsbA and were found to stimulate the ATPase activity of the detergent-purified transporter about 2-fold in the absence (41) and 3–4 fold in complex with DARPin_55. This implies that drug-in-

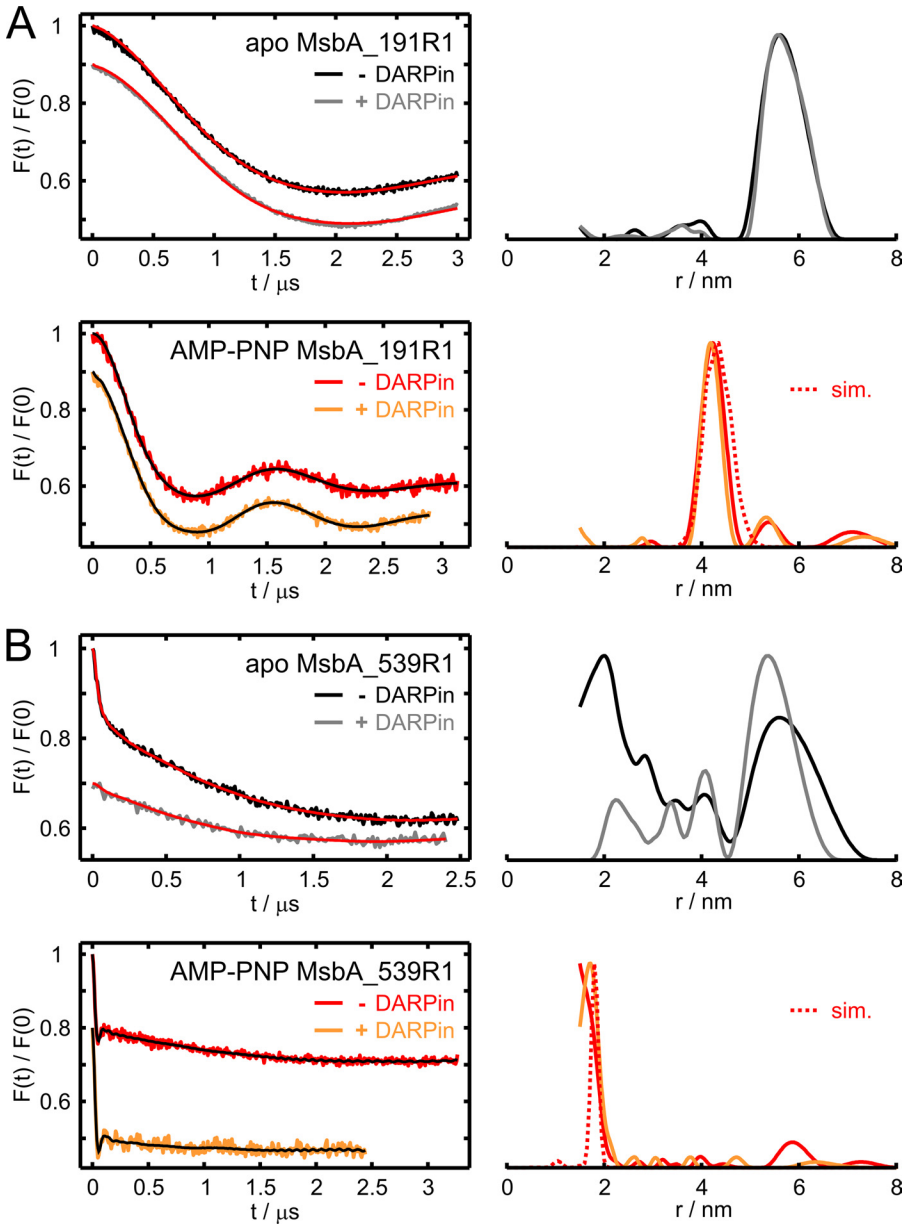

FIGURE 2. **Intra-MsbA distance measurements by DEER reveal no major conformational changes of the transporter upon binding of wild-type DARPin.** *A*, *left*, normalized DEER form factors F(t) and fits obtained with DeerAnalysis2010 on detergent-purified MsbA_191R1 alone and in complex with wild-type DARPin_55. Traces were detected in the apo-state and in the AMP-PNP-state (5 mM AMP-PNP and 5 mM $MgCl_2$) in the absence and in the presence of DARPin_55, as indicated. *Right*, distance distributions obtained with Tikhonov regularization parameters 100 or 1000. The intra-MsbA distances simulated based on the AMP-PNP x-ray structure (PDB 3B60) are superimposed (*red dotted*). *B*, DEER analysis on MsbA_539R1 alone and in complex with DARPin_55 analogous to *A*.

duced and DARPin_55-mediated stimulations of the basal ATPase activity of MsbA are additive (Fig. 1, *E* and *F*). Therefore, DARPin binding does not appear to interfere with MsbA's capability to bind its cargo substrates. MsbA and the MsbA_E506Q (42) mutant (whose ATPase activity is abolished) were reconstituted in proteoliposomes (34). The addition of lipid A and daunomycin stimulate the ATPase activity of reconstituted MsbA about 2-fold as described previously (supplemental Fig. S6) (41). In contrast to detergent-purified MsbA the basal ATPase activity of reconstituted MsbA was not stimulated by the addition of DARPin_55, because DARPin_55 does not bind to membrane-embedded MsbA as discussed below (supplemental Fig. S7).

Binding of DARPin Does Not Impair MsbA Ability to Undergo Conformational Changes—To study the possible structural effects induced by DARPin binding to the transporter, single cysteine mutants of MsbA were labeled with MTSSL and interspin distances between the two labeled sites were measured by DEER in the apo- and AMP- PNP- stsates. The DEER analysis on two representative spin-labeled sites (position 191 in the TMDs and position 539 in the NBDs) is presented in Fig. 2. The 191–191 distance in the apo-state centered at 5.8 nm was found to be in line with the apo crystal structure (9), showing a C_α-C_α distance of 4.7 nm. The distance decreased to 4.1 nm upon addition of AMP-PNP and $MgCl_2$ (Fig. 2*A*), which fully agrees with the interspin distance simulated with the program MMM

(38) based on the AMP-PNP structure of MsbA. Upon complex formation with DARPin_55, MsbA showed the same distance distributions, indicating that the detergent-solubilized MsbA retained the ability to accomplish the conformational changes induced by nucleotide binding (Fig. 2*A*).

The AMP-PNP-state exhibited a sharp 1.8 nm distance between the two 539 labels located in the NBDs, both in the absence and presence of DARPin_55 (Fig. 2*B*). The obtained distance is again in perfect agreement with the crystallographic data, strongly indicating that DARPin binding does not lead to major structural changes in MsbA. The apo-state of the 539 mutant of MsbA showed a peak at about 6 nm in line with the inverted V-shaped apo crystal structure, which is characterized by a C_α-C_α distance of 6.4 nm. A second broad peak between 2 and 4 nm was present which might represent intermediate conformations adopted during NBD closure or disengagement. However, these intermediate states were only observed in this particular mutant and they were strongly suppressed after reconstitution into liposomes (supplemental Fig. S6). Interestingly, adding DARPin_55 to the apo-state of the 539 mutant of MsbA diminished the short distances but did not affect the 6 nm peak suggesting a stabilization of the open-apo structure by DARPin_55 in analogy to the reconstitution into liposomes (Fig. 2*B*, supplemental Fig. S6). Taking into consideration all tested mutants, the inverted V-shaped crystal structure and the outward-facing AMP-PNP bound structure (9) appear to describe the conformational changes of detergent-solubilized MsbA appropriately.

DARPin_55 Binds to the Transmembrane Domain of Detergent-purified MsbA—To delineate the binding epitope of DARPin_55 on full-length MsbA we used purified sub-domains of MsbA, namely the TMD and the NBD. For this purpose, the domains were purified as Avi-tagged biotinylated proteins ($bTMD_{AviC}$ and $bNBD_{AviC}$) and binding to DARPin_55 was assessed by the same ELISA setup as used to identify MsbA-specific DARPins described above (Fig. 1*B*, supplemental Fig. S2). This ELISA experiment revealed that DARPin_55 binds to the transmembrane domain ($bTMD_{AviC}$) but not to the nucleotide binding domain ($bNBD_{AviC}$) of MsbA. Binding of DARPin_55 to $bTMD_{AviC}$ resulted in a comparatively smaller ELISA signal than binding to full length $bMsbA_{AviC}$. This could be due to partially unstructured regions on the TMDs in the absence of the NBDs. Binding of DARPin_55 was further tested using membrane vesicles containing overexpressed MsbA and MsbA reconstituted in proteoliposomes (supplemental Fig. S7). In contrast to detergent-purified MsbA, DARPin_55 did not bind to the membrane-embedded transporter indicating that the binding epitope on MsbA cannot be accessed by DARPin_55 because it is (at least partially) masked by the lipid bilayer.

Cysteine Cross-linking of DARPin and MsbA Mutants—To further specify the binding epitope of DARPin_55 on MsbA, single cysteines were introduced into MsbA and DARPin_55 and proximities between these cysteines were detected using the thiol-specific homobifunctional cross-linkers M5M and M11M. A total of nine single cysteine mutants were made at different positions in the cytoplasmic part of the TMD of MsbA and in DARPin_55 (four in MsbA at positions 103, 191, 206, and 246 and five in DARPin_55 at positions 12, 16, 29, 151, and 160). Using ELISA, each mutated DARPin was confirmed to bind to every single cysteine MsbA mutant (data not shown). All possible combinations of MsbA and DARPin_55 cysteines mutants were then cross-linked as described in the experimental procedures. The single cysteine mutants of MsbA alone did not form any cross-linked products in the presence of M11M and M5M (Fig. 3*A*) nor could any of the DARPin mutants be cross-linked to Cys-less MsbA (supplemental Fig. S8). Cysteines introduced at the N terminus of DARPin_55 (at positions 12, 16, and 29) were efficiently cross-linked to MsbA_191C and to a lesser extent to MsbA_206C and MsbA_246C with both cross-linkers (supplemental Fig. S8). MsbA_103C formed only faint cross-linking products with all DARPin mutants tested. Likewise, the cysteines at the C terminus of DARPin_55 (at positions 151 and 160) were only poorly cross-linked with the four MsbA single cysteine mutants with either cross-linker. These faint cross-linking products seemed promiscuous and were therefore considered as background. In summary, the N terminus of DARPin_55 is in close proximity to the MsbA_191C position whereas the orientation of the C-terminal part of DARPin_55 could not be resolved by only this analysis.

One Molecule of DARPin_55 Binds to the MsbA Homodimer—The maximal degree of DARPin cross-linking to MsbA never seemed to exceed 50% of the MsbA chains (supplemental Fig. S8). To further investigate this phenomenon, cross-linking between DARPin_55_29C and MsbA_191C was carried out in the absence of nucleotides as well as in the presence of AMP-PNP or ATP-vanadate using increasing amounts of DARPin (Fig. 3). Interestingly, cross-linking was saturated at a stoichiometry of approximately one DARPin binding to homodimeric MsbA in its apo-state (Fig. 3*A*). The exact stoichiometry was quantified by SYPRO Ruby staining to 0.73 $\pm$ 0.01 DARPins cross-linked to MsbA (Fig. 4*A*). The presence of AMP-PNP or ATP-vanadate appears to diminish the cross-linking reaction (Fig. 3, *B* and *C*), which might be caused by a longer distance between the thiol groups in this state (see EPR data below) and/or a decreased binding affinity of the DARPin for the nucleotide-bound state(s) of MsbA. Despite multiple attempts, we were not able to perform surface plasmon resonance (SPR) measurements which would have allowed for the determination of binding constants of DARPin_55 recognizing different conformational states of MsbA. The ATPase activity of the DARPin_55_29C/MsbA_191C complex is stimulated by a factor of two compared with MsbA_191C alone and remains unchanged upon cross-linking using M11M (Fig. 3*D*). This indicates that the DARPin_55 remains bound to MsbA during its entire catalytic cycle. Binding stoichiometries were further studied by gel filtration experiments. The MsbA/DARPin_55 complex was separated from excess DARPin_55 by size-exclusion chromatography (supplemental Fig. S4) followed by a quantitative analysis of DARPin_55 and MsbA using the protein chip technology (Agilent Technologies) (supplemental Fig. S9). In agreement with the cross-linking results, the ratio between DARPin_55 and MsbA dimer was quantified to 0.8. The binding stoichiometries in the gel filtration assay as well as in the cross-linking experiment were slightly less than one DARPin bound per MsbA dimer. For the gel filtration assay, this is likely due to partial dissociation of DARPin_55 from

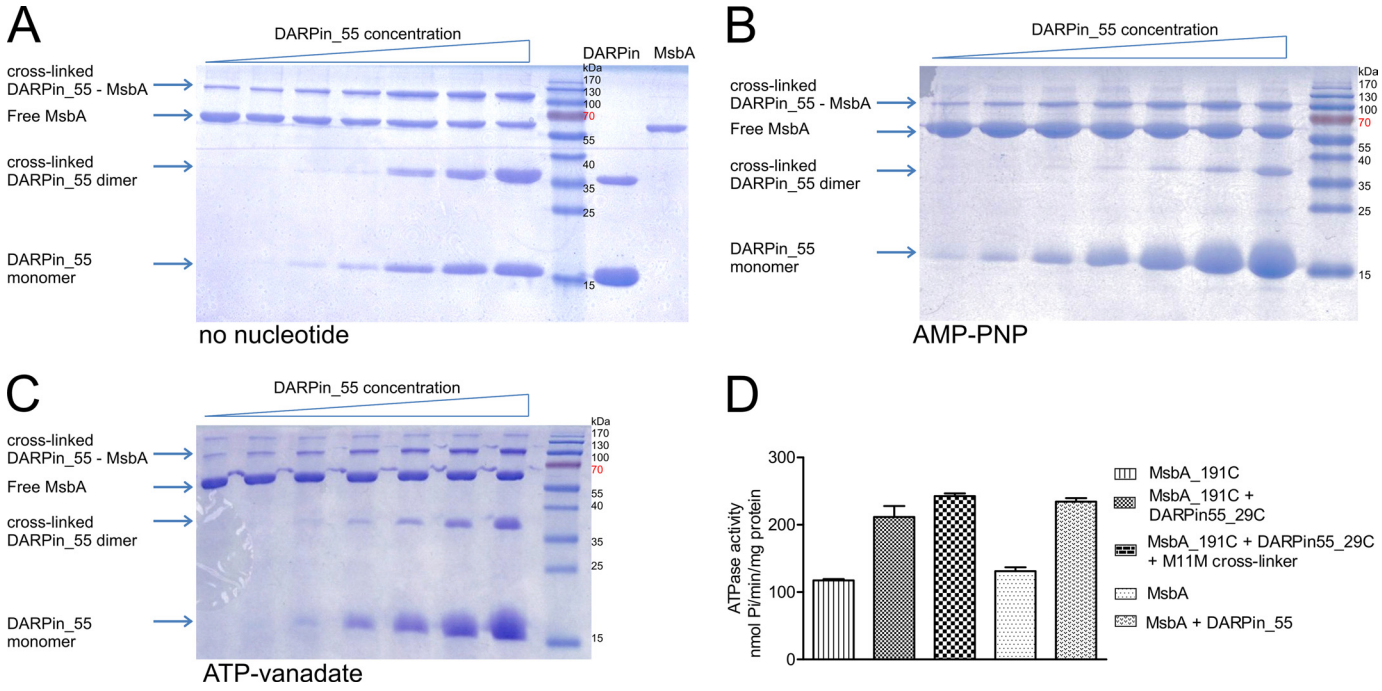

FIGURE 3. **Methanethiosulfonate-mediated cross-linking of one DARPin to homodimeric MsbA.** *A–C*, MsbA_191C (1 μM) was incubated with increasing amounts of DARPin_55_29C (from 500 nM to 16 μM) in the absence of nucleotides *A*, in the presence of $MgCl_2$ (3.5 mM) and AMP-PNP (3 mM) *B*, or ATP-vanadate (2.5 mM, each). *C*, protein complexes were cross-linked using the homobifunctional M11M cross-linker (2 mM) for 15 min at 4 °C and separated by non-reducing SDS-PAGE. *D*, ATPase activities of cross-linked MsbA191C-DARPin_55_29C complexes are equal to those of non-treated MsbA-DARPin complexes and are consistently increased by a factor of two compared with MsbA alone.

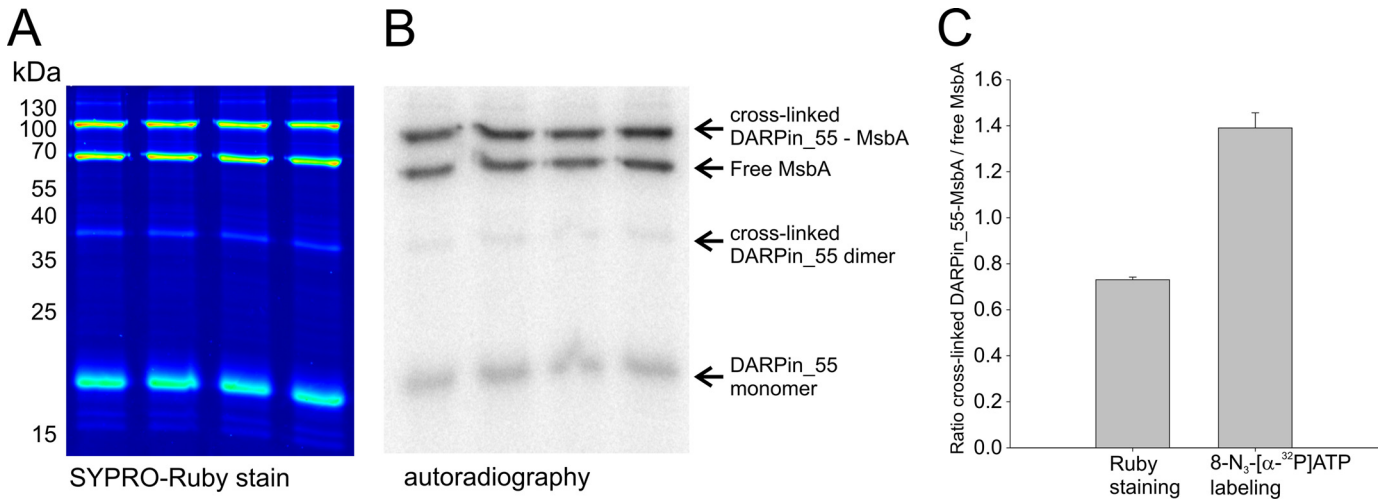

FIGURE 4. **Preferential nucleotide binding to one chain of asymmetrically stabilized MsbA as determined by 8-N_3-[α-^{32}P]ATP photolabeling.** *A* and *B*, DARPin_55_29C was cross-linked to MsbA_191C using M11M, followed by addition of 8-N_3-[α-^{32}P]ATP (1 μM) and UV-cross-linking (performed as quadruplicates). The samples were separated by non-reducing SDS-PAGE and analyzed by SYPRO Ruby staining *A* and autoradiography *B*. *C*, band intensities corresponding to cross-linked DARPin-MsbA complex and free MsbA monomer obtained in *A* and *B* were quantified.

MsbA during the size-exclusion run whereas in the cross-linking experiment, some of the thiol moieties of the cysteines might have undergone oxidation during the purification and as a consequence would not react with the methanethiosulfonate cross-linker. At this point, two scenarios can explain the binding stoichiometry of one DARPin bound per homodimeric MsbA: (i) Binding of the first DARPin molecule to MsbA sterically prevents binding of the second or (ii) the DARPin recognizes asymmetries in MsbA.

EPR Distances between DARPin_55 and MsbA—To rule out possible steric clashes between the two DARPins in the complex, the binding epitope of DARPin_55 on MsbA was mapped by EPR. Various combinations of five spin-labeled single cysteine mutants spanning the MsbA structure (positions 25, 65, 103, 191, 482) and two spin-labeled DARPin_55 (positions 29 or 160) were measured to extract interspin distances by DEER.

Because of the 1:1 stoichiometric ratio between DARPin_55 and MsbA, binding of one spin-labeled DARPin to the homodimeric spin-labeled transporter gives rise to a three-spin complex. This was confirmed by measuring the spin concentration in the MsbA-DARPin complexes using continuous wave EPR (data not shown). To disentangle the intra-MsbA from the

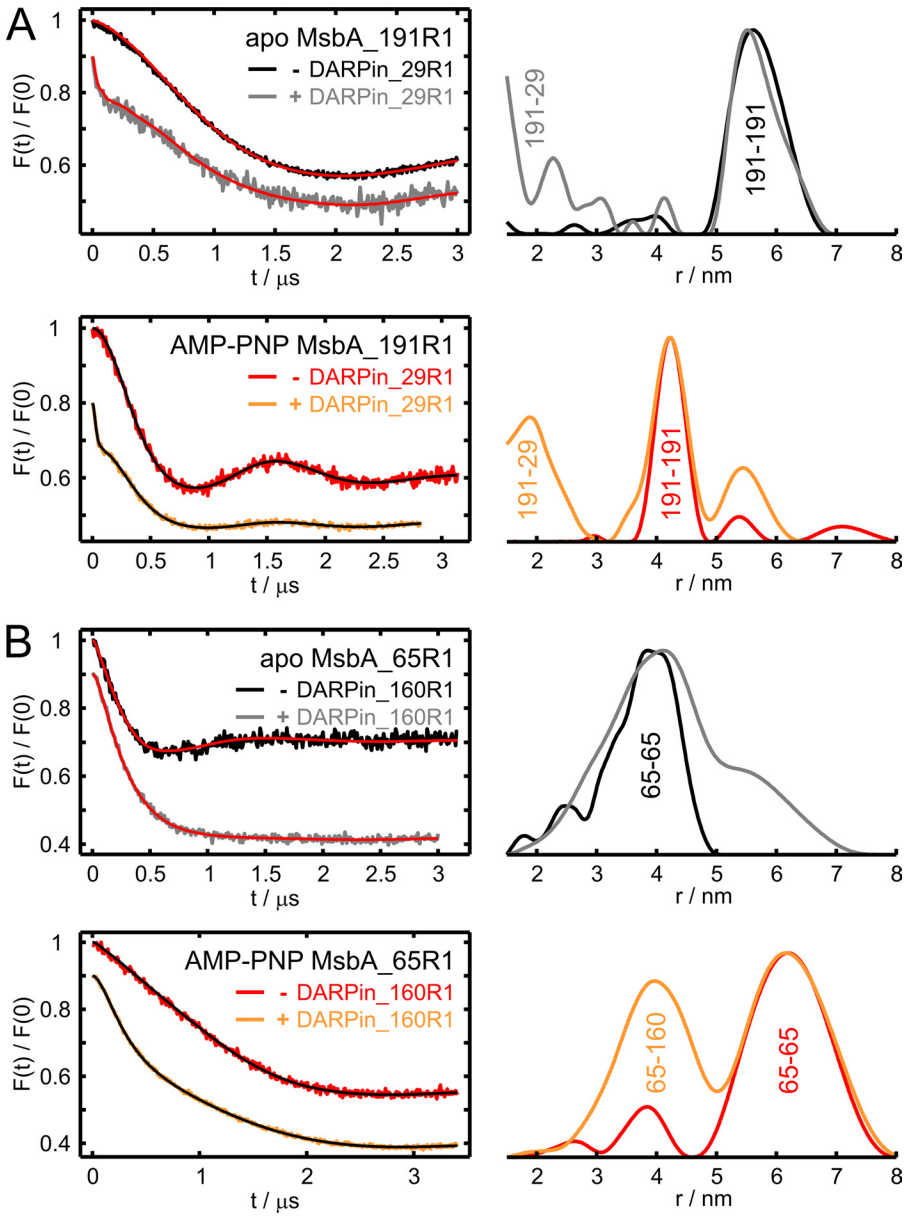

FIGURE 5. **Determination of the binding epitope of DARPin_55 by DEER.** *A*, *left*, normalized DEER form factors F(t) and fits obtained with DeerAnalysis2010 on detergent-purified MsbA_191R1 alone and in complex with DARPin_55 spin labeled at position 29 (N-cap). Traces were detected in the apo-state and in the AMP-PNP-state (5 mM AMP-PNP and 5 mM $MgCl_2$) in the absence and in the presence of DARPin_55_29R, as indicated. *Right*, distance distributions obtained with Tikhonov regularization parameters 100 or 1000. Assigned MsbA-DARPin distances are marked in the distance distribution. *B*, DEER analysis on MsbA_65R1 alone and in complex with DARPin_55 spin labeled at position 160 (C-cap) analogous to *A*. The vicinity of the intra-MsbA and DARPin-MsbA distances in the apo-state prevented a clear assignment of the DEER constraint.

MsbA-DARPin distances, we measured the MsbA alone and in the presence of the DARPin. To reduce the known effects of three-spin artifacts in the distance distributions (44), the intra-MsbA and the MsbA-DARPin distances should be as distinct as possible.

Among all combinations tested, only two (MsbA_191R1-DARPin_55_29R1 and MsbA_65R1-DARPin_55_160R1, with R1 denoting the MTSSL spin-labeled side chain) resulted in extractable MsbA-DARPin distances (Fig. 5) (all DEER distances are presented in Fig. 6). The intra-MsbA_191R1 distances in the apo- and AMP-PNP- states are shown in Fig. 5*A*. Addition of DARPin_55_29R1 resulted in the appearance of a short distance peak at 1.5–2 nm confirming the close proximity of the N-terminal region (N-cap) of DARPin_55 to position 191 in the TMDs already observed by cross-linking (supplemental Fig. S8). Interestingly, the distance between these two positions becomes slightly longer (~2 nm) in the presence of AMP-PNP. In agreement with the DEER results obtained with unlabeled DARPin_55 (Fig. 2*A*), the intra-MsbA_191R1 distance remains unchanged upon addition of DARPin_55_29R1 in the apo-state and in the presence of AMP-PNP (Fig. 5*A*). The longer distance observed between the two nitroxide labels in MsbA and DARPin_55 might explain the reduced degree of M11M mediated cross-linking observed upon addition of nucleotides (Fig. 3, *B* and *C*).

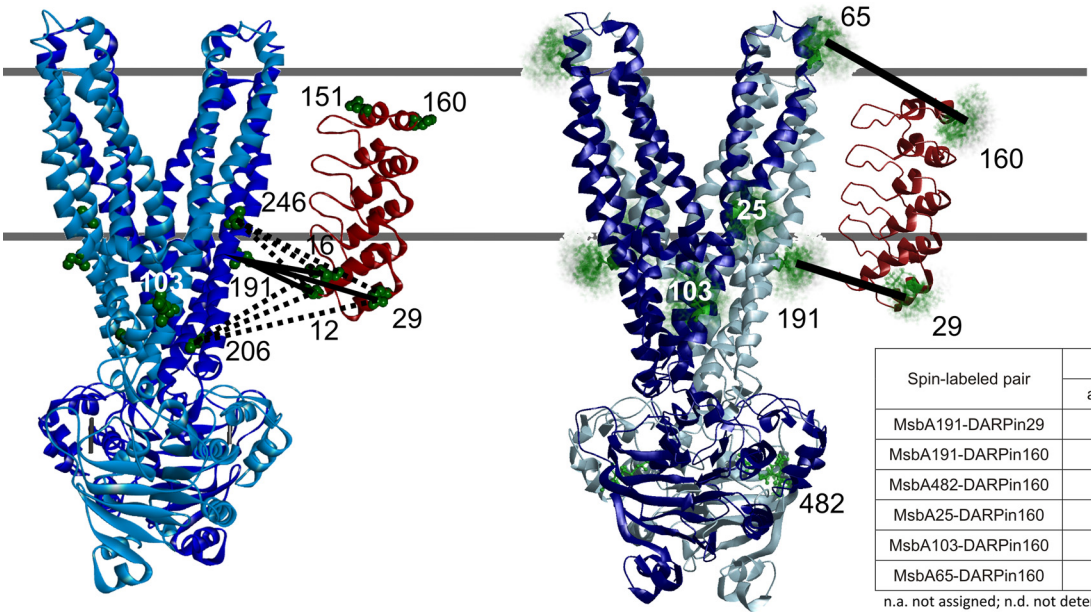

Spin-labeled pair	MsbA-DARPin distance	
	apo state	AMP-PNP
MsbA191-DARPin29	~ 2 nm	~ 2 nm
MsbA191-DARPin160	> 5 nm	n.d.
MsbA482-DARPin160	> 7 nm	n.d.
MsbA25-DARPin160	> 6 nm	n.d.
MsbA103-DARPin160	> 6 nm	n.d.
MsbA65-DARPin160	n.a.	3.9 nm

n.a. not assigned; n.d. not determined.

FIGURE 6. **The MsbA-DARPin complex based on cross-linking and DEER data.** *A*, overview of the cross-linking data (supplemental Fig. S8) using the x-ray structure of MsbA (PDB 3B60) and a homology model of DARPin_55 as templates. The *black straight lines* indicate thiol pairs showing strong cross-links, the *black dotted lines* denote pairs showing weak cross-links. *B*, overview of interspin distances between MsbA and DARPin_55. The possible spin label rotamers attached at selected positions in MsbA were simulated using the Matlab program package MMM and are indicated as *green clouds*. The *black straight lines* highlight the pairs for which DEER constraints were obtained. All DEER data including the restraints are presented in the table.

Whereas the position of the N-cap of DARPin_55 with respect to the TMD could be readily mapped by cross-linking and EPR, the orientation of the DARPin's C-cap was challenging to find, also because no cross-link could be established between the 151 and 160 positions of DARPin_55 and any of the MsbA mutants used (supplemental Fig. S8). After screening by DEER a number of complexes with DARPin_55 labeled at the C-cap (position 160), we found a clear distance constraint between the C-cap and the extracellular region of the transporter (position 65). In aggrement with the structural changes expected from the x-ray data, addition of AMP-PNP to isolated MsbA resulted in an increase of the 65–65 distance from 4 to 6 nm (Fig. 4*B*). When DARPin_55_160R1 was analyzed in complex with MsbA_65R1, we found a distinct MsbA-DARPin_55 distance centered at 3.9 nm in the AMP-PNP-state, while the overlap with the intra-MsbA distance prevented a clear MsbA-DARPin_55 distance assignment in the apo-state. In contrast, we could exclude distances < 5 nm between the C-cap of DARPin_55 and other spin labels in the NBDs (position 482) and in the cytoplasmic-facing region of the TMDs (positions 25, 103, 191) (Fig. 6). Based on these observations we could rule out that the C-cap is oriented toward the NBDs, thus the transmembrane domain of MsbA seems to be covered at least partially by DARPin_55. Importantly, the DARPin binding epitope was found to be far away from the 2-fold symmetry axis of MsbA, thus ruling out the possibility of steric clashes between two DARPins as the cause for the stoichiometric ratio observed.

The ATPase Sites of Asymmetrically Stabilized MsbA Display Different Nucleotide Binding Properties—Cross-linking DARPin_55_29C to asymmetric MsbA_191C provides the unprecedented advantage that the conformationally unequal chains of homodimeric MsbA can be separated by SDS-PAGE. Thus questions as whether the two ATPase sites of asymmetric MsbA display differences with respect to nucleotide binding can be for the first time addressed. The cross-linked DARPin-MsbA complex was incubated with 8-N_3-[α-^{32}P]ATP followed by UV cross-linking of the nucleotide to the two chains of MsbA. Subsequently, the proteins were separated by SDS-PAGE and the amount of cross-linking was determined by autoradiography (Fig. 4). The ratio between the bands of DARPin_55 cross-linked to MsbA and MsbA alone was quantified to be 0.73 $\pm$ 0.01 by SYPRO Ruby staining. Interestingly, the MsbA chain cross-linked to DARPin_55 showed a stronger photolabeling with 8-N_3-[α-^{32}P]ATP than the MsbA chain alone (ratio between MsbA-DARPin_55 to MsbA of 1.39 $\pm$ 0.07). This indicates that the MsbA monomer to which the DARPin was cross-linked to was photolabeled 1.9 times stronger than the free MsbA chain.

DISCUSSION

Asymmetries in the NBDs of ABC exporters arising from trapping of nucleotides by vanadate have been discussed since the mid-nineties when Urbatsch and Senior first described the catalytic cycle of P-glycoprotein and later were also found in the homodimeric transporter BmrA (16, 17). Using an *in vitro* selected DARPin binder, we provide here novel evidence supporting considerable asymmetries to be found in a well-studied ABC exporter.

Our biochemical analysis shows that DARPin_55 binds to the TMDs of MsbA in a stoichiometry of one DARPin per homodimeric transporter. The binding epitope was mapped to the TMDs of MsbA and therefore, the possibility that binding of the first DARPin sterically hinders binding of a second DARPin to the symmetry-related epitope on MsbA could be excluded. In further support of this notion, DARPin binding does not affect the closure of the NBDs and the transition to the

outward-facing state of MsbA upon addition of AMP-PNP. The DARPin therefore recognizes asymmetries in MsbA.

Asymmetric homodimers are not unusual. The epidermal growth factor receptor from *Drosophila* has been recently crystallized in an asymmetric state in complex with two growth factor ligands binding in a low- and a high-affinity mode (45). Caspase-9 is activated by dimerization and was crystallized as asymmetric homodimer exhibiting one active and one inactive catalytic site (46). However, despite serious efforts we did not succeed to solve the co-crystal structure of the MsbA-DARPin_55 complex and therefore the molecular details of the asymmetries in MsbA remain elusive.

Epitope mapping revealed that the DARPin binding site includes membrane-spanning portions of the TMD (Fig. 6). There are two observations which further support this unexpected finding. First, DARPin_55 only binds to MsbA in its detergent-purified but not in its membrane-bound form (supplemental Fig. S7). In a detergent-purified MsbA sample, free detergent monomers, protein-free detergent micelles and detergent bound to the membrane protein are in equilibrium (47). There is constant rapid exchange of detergents molecules between these pools. Lipid bilayers in contrast are more rigid (48). It is therefore likely that DARPin_55 partly displaces the detergent micelle, but not the relatively stiffer lipid membrane to bind to its epitope. Second, in agreement with the positioning of DARPin_55 with respect to the membrane boundary, the randomized positions in the β-turns of the second and the third DARPin repeat exclusively harbor hydrophobic amino acids (supplemental Fig. S10). These residues could mediate hydrophobic contacts with the transmembrane helices of MsbA, whereas in the first repeat, there are two glutamates which could interact with the cytoplasmic portion of the TMD. Importantly, DARPin_55 only recognizes MsbA, but not its homologue LmrCD or the multidrug transporter AcrB. Therefore, unspecific hydrophobic interactions of DARPin_55 with membrane proteins in general can be excluded. Interestingly, the presence of DARPin_55 increased the ATPase activity of the β-UDM-solubilized transporter by influencing the V_{max} term, independent of the substrate-induced stimulations. This finding is reminiscent of a recent biochemical characterization of the P-glycoprotein-specific antibody MRC16 the addition of which was found to increase the ATPase activity of the transporter in the absence as well as in the presence of the substrate nicardipine (49).

It has often been argued that *in vitro* selected binding proteins may distort the target protein thereby trapping it in an unnatural and non-physiological state. However, numerous examples of crystal structures solved alone and in complex with a binding partner in very similar conformations speak against this argument (as reviewed in Refs. 24, 50, 51). One prominent example reminiscent to the study presented here is the homotrimeric multidrug transporter AcrB, that has been crystallized alone and in complex with DARPins in an asymmetric conformation in which each conformer represents a consecutive step of the transport cycle (25, 27, 28). Only two DARPins were found to bind to the trimer, and at the third expected DARPin binding site, a steric clash between a conformationally altered subdomain of AcrB with the back side of the DARPin prevented binding (25, 26). The DARPins did not induce the asymmetric state, but rather recognized the intrinsic asymmetry of the targeted protein. It is therefore plausible that the asymmetric conformational states of MsbA to which DARPin_55 binds to belong to the intrinsic ensemble of possible conformations of the transporter.

DEER and cross-linking experiments show that DARPin_55 binds to homodimeric MsbA in the apo-state as well as in the presence of AMP-PNP and ATP-vanadate and therefore the recognized asymmetries in MsbA do not appear to be state-specific. In support of this notion, cross-linked MsbA-DARPin complexes retain their increased ATPase activity suggesting that the DARPin remains bound during the entire catalytic cycle. Importantly, DARPin binding does not trap MsbA in an asymmetric state, which would lead to an inhibition of the ATPase activity, but rather enables the transporter to interconvert between conformations necessary for function at a higher rate. Our findings stand in partial contrast to a recent study on P-glycoprotein antibodies MRK16 and UIC2, which were shown to bind to the transporter in the apo-state as well as in the presence of AMP-PNP (pre-hydrolytic state), but not if the transporter is trapped with ADP-vanadate (post-hydrolytic state) (49). In addition to earlier studies dealing with the asymmetric nature of the catalytic cycle at the NBDs (16, 17), our results indicate that distinct asymmetries also inhere to the TMDs of MsbA where the DARPin_55 epitope is located. Lipid A, the natural substrate of MsbA, is rather big (molecular weight of around 1.8 kDa) and asymmetric. Therefore, it is plausible to assume that only one molecule of lipid A can be accommodated by the substrate binding cavity of MsbA which might require asymmetries in the TMDs. We found that the ATPase activity of detergent-purified MsbA was stimulated by lipid A and daunomycin. Our observations with lipid A agree with a previous study (41), although the stimulation observed by us is not as pronounced as reported, whereas in the same study stimulation of the ATPase by daunomycin was not apparent. These differences might arise from the different detergents used for purification of MsbA (β-UDM in our case and β-DM in the mentioned study (41)). Interestingly, the stimulation of MsbA's ATPase activity by lipid A or daunomycin and DARPin_55 are additive (Fig. 1, *D* and *E*). DARPin binding therefore does not seem to interfere with substrate interactions at the binding cavity. 8-N_3-[α-^{32}P]ATP was shown to preferentially photolabel one of the chains of asymmetric homodimeric MsbA, hence supporting the notion that the asymmetries recognized by the DARPin at the TMDs are conformationally linked to the nucleotide binding sites at the NBDs and *vice versa*. Since photocross-linking using 8-N_3-[α-^{32}P]ATP is a non-equilibrium binding method, further biochemical analyses are difficult. Nevertheless, in symmetric MsbA both nucleotide binding sites are identical and expected to be labeled by equal amounts of 8-N_3-[α-^{32}P]ATP. This is not the case and therefore, the two nucleotide binding sites are different from each other. As previously proposed based on biochemical experiments and molecular dynamics simulations, the asymmetric switching at the NBDs might be a prerequisite for ATP hydrolysis (16, 17, 19, 21). Our data suggest that DARPin binding to MsbA populates asymmetric states of the transporter from an

ensemble of structurally similar conformations which exhibits increased basal ATPase activities and is fully compatible with its function to bind lipid A and drugs.

Acknowledgment—We thank Michael Hohl for valuable discussions.

REFERENCES

1. Holland, I. B. (2011) ABC transporters, mechanisms and biology: an overview. *Essays Biochem.* **50,** 1–17
2. Zhou, Z., White, K. A., Polissi, A., Georgopoulos, C., and Raetz, C. R. (1998) Function of *Escherichia coli* MsbA, an essential ABC family transporter, in lipid A and phospholipid biosynthesis. *J. Biol. Chem.* **273,** 12466–12475
3. Polissi, A., and Georgopoulos, C. (1996) Mutational analysis and properties of the msbA gene of *Escherichia coli*, coding for an essential ABC family transporter. *Mol. Microbiol.* **20,** 1221–1233
4. van Veen, H. W., Venema, K., Bolhuis, H., Oussenko, I., Kok, J., Poolman, B., Driessen, A. J., and Konings, W. N. (1996) Multidrug resistance mediated by a bacterial homolog of the human multidrug transporter MDR1. *Proc. Natl. Acad. Sci. U.S.A.* **93,** 10668–10672
5. Aller, S. G., Yu, J., Ward, A., Weng, Y., Chittaboina, S., Zhuo, R., Harrell, P. M., Trinh, Y. T., Zhang, Q., Urbatsch, I. L., and Chang, G. (2009) Structure of P-glycoprotein reveals a molecular basis for poly-specific drug binding. *Science* **323,** 1718–1722
6. Reuter, G., Janvilisri, T., Venter, H., Shahi, S., Balakrishnan, L., and van Veen, H. W. (2003) The ATP-binding cassette multidrug transporter LmrA and lipid transporter MsbA have overlapping substrate specificities. *J. Biol. Chem.* **278,** 35193–35198
7. Woebking, B., Reuter, G., Shilling, R. A., Velamakanni, S., Shahi, S., Venter, H., Balakrishnan, L., and van Veen, H. W. (2005) Drug-lipid A interactions on the *Escherichia coli* ABC transporter MsbA. *J. Bacteriol.* **187,** 6363–6369
8. Dawson, R. J., and Locher, K. P. (2006) Structure of a bacterial multidrug ABC transporter. *Nature* **443,** 180–185
9. Ward, A., Reyes, C. L., Yu, J., Roth, C. B., and Chang, G. (2007) Flexibility in the ABC transporter MsbA: Alternating access with a twist. *Proc. Natl. Acad. Sci. U.S.A.* **104,** 19005–19010
10. Zou, P., Bortolus, M., and McHaourab, H. S. (2009) Conformational cycle of the ABC transporter MsbA in liposomes: detailed analysis using double electron-electron resonance spectroscopy. *J. Mol. Biol.* **393,** 586–597
11. Smriti, Zou, P., and McHaourab, H. S. (2009) Mapping daunorubicin-binding sites in the ATP-binding cassette transporter MsbA using site-specific quenching by spin labels. *J. Biol. Chem.* **284,** 13904–13913
12. Borbat, P. P., Surendhran, K., Bortolus, M., Zou, P., Freed, J. H., and McHaourab, H. S. (2007) Conformational motion of the ABC transporter MsbA induced by ATP hydrolysis. *PLoS Biol.* **5,** e271
13. Zou, P., and McHaourab, H. S. (2009) Alternating access of the putative substrate-binding chamber in the ABC transporter MsbA. *J. Mol. Biol.* **393,** 574–585
14. Doshi, R., Woebking, B., and van Veen, H. W. (2010) Dissection of the conformational cycle of the multidrug/lipidA ABC exporter MsbA. *Proteins* **78,** 2867–2872
15. Procko, E., O'Mara, M. L., Bennett, W. F., Tieleman, D. P., and Gaudet, R. (2009) The mechanism of ABC transporters: general lessons from structural and functional studies of an antigenic peptide transporter. *FASEB J.* **23,** 1287–1302
16. Urbatsch, I. L., Sankaran, B., Weber, J., and Senior, A. E. (1995) P-glycoprotein is stably inhibited by vanadate-induced trapping of nucleotide at a single catalytic site. *J. Biol. Chem.* **270,** 19383–19390
17. Orelle, C., Dalmas, O., Gros, P., Di Pietro, A., and Jault, J. M. (2003) The conserved glutamate residue adjacent to the Walker-B motif is the catalytic base for ATP hydrolysis in the ATP-binding cassette transporter BmrA. *J. Biol. Chem.* **278,** 47002–47008
18. Senior, A. E., al-Shawi, M. K., and Urbatsch, I. L. (1995) The catalytic cycle of P-glycoprotein. *FEBS Lett.* **377,** 285–289
19. Zaitseva, J., Oswald, C., Jumpertz, T., Jenewein, S., Wiedenmann, A., Holland, I. B., and Schmitt, L. (2006) A structural analysis of asymmetry required for catalytic activity of an ABC-ATPase domain dimer. *EMBO J.* **25,** 3432–3443
20. Dawson, R. J., and Locher, K. P. (2007) Structure of the multidrug ABC transporter Sav1866 from *Staphylococcus aureus* in complex with AMP-PNP. *FEBS Lett.* **581,** 935–938
21. Aittoniemi, J., de Wet, H., Ashcroft, F. M., and Sansom, M. S. (2010) Asymmetric switching in a homodimeric ABC transporter: a stimulation study. *PLoS Comput. Biol.* 6, e1000762
22. Gyimesi, G., Ramachandran, S., Kota, P., Dokholyan, N. V., Sarkadi, B., and Hegedus, T. (2011) ATP hydrolysis at one of the two sites in ABC transporters initiates transport related conformational transitions. *Biochim. Biophys. Acta* **1808,** 2954–2964
23. Binz, H. K., Amstutz, P., Kohl, A., Stumpp, M. T., Briand, C., Forrer, P., Grütter, M. G., and Plückthun, A. (2004) High-affinity binders selected from designed ankyrin repeat protein libraries. *Nat. Biotechnol.* **22,** 575–582
24. Sennhauser, G., and Grütter, M. G. (2008) Chaperone-assisted crystallography with DARPins. *Structure* **16,** 1443–1453
25. Sennhauser, G., Amstutz, P., Briand, C., Storchenegger, O., and Grütter, M. G. (2007) Drug export pathway of multidrug exporter AcrB revealed by DARPin inhibitors. *Biol.* **5,** e7
26. Monroe, N., Sennhauser, G., Seeger, M. A., Briand, C., and Grütter, M. G. (2011) Designed ankyrin repeat protein binders for the crystallization of AcrB: plasticity of the dominant interface. *J. Struct. Biol.* **174,** 269–281
27. Murakami, S., Nakashima, R., Yamashita, E., Matsumoto, T., and Yamaguchi, A. (2006) Crystal structures of a multidrug transporter reveal a functionally rotating mechanism. *Nature* **443,** 173–179
28. Seeger, M. A., Schiefner, A., Eicher, T., Verrey, F., Diederichs, K., and Pos, K. M. (2006) Structural asymmetry of AcrB trimer suggests a peristaltic pump mechanism. *Science* **313,** 1295–1298
29. Huber, T., Steiner, D., Röthlisberger, D., and Plückthun, A. (2007) *In vitro* selection and characterization of DARPins and Fab fragments for the co-crystallization of membrane proteins: The Na(+)-citrate symporter CitS as an example. *J. Struct. Biol.* **159,** 206–221
30. Zahnd, C., Amstutz, P., and Plückthun, A. (2007) Ribosome display: selecting and evolving proteins *in vitro* that specifically bind to a target. *Nat. Methods* **4,** 269–279
31. Deleted in proof
32. Loo, T. W. (2001) Determining the dimensions of the drug-binding domain of human P-glycoprotein using thiol cross-linking compounds as molecular rulers. *J. Biol. Chem.* **276,** 36877–36880
33. Venter, H., Velamakanni, S., Balakrishnan, L., and van Veen, H. W. (2008) On the energy-dependence of Hoechst 33342 transport by the ABC transporter LmrA. *Biochem. Pharmacol.* **75,** 866–874
34. Geertsma, E. R., Nik Mahmood, N. A., Schuurman-Wolters, G. K., and Poolman, B. (2008) Membrane reconstitution of ABC transporters and assays of translocator function. *Nat. Protoc.* **3,** 256–266
35. Pannier, M., Veit, S., Godt, A., Jeschke, G., and Spiess, H. W. (2000) Dead-time free measurement of dipole-dipole interactions between electron spins. *J. Magn Reson* **142,** 331–340
36. Forrer, J., García-Rubio, I., Schuhmam, R., Tschaggelar, R., and Harmer, J. (2008) Cryogenic Q-band (35GHz) probehead featuring large excitation microwave fields for pulse and continuous wave electron paramagnetic resonance spectroscopy: performance and applications. *J. Magn Reson* **190,** 280–291
37. Jeschke, G., Chechik, V., Ionita, P., Godt, A., Zimmermann, H., Banham, J., Timmel, C. R., Hilger, D., and Jung, H. (2006) DeerAnalysis2006 - a comprehensive software package for analyzing pulsed ELDOR data. *Appl. Magn. Res.* **30,** 473–498
38. Polyhach, Y., Bordignon, E., and Jeschke, G. (2011) Rotamer libraries of spin labelled cysteines for protein studies. *Phys. Chem. Chem. Phys.* **13,** 2356–2366
39. Binz, H. K., Stumpp, M. T., Forrer, P., Amstutz, P., and Plückthun, A. (2003) Designing repeat proteins: well-expressed, soluble and stable proteins from combinatorial libraries of consensus ankyrin repeat proteins. *J. Mol. Biol.* **332,** 489–503
40. Kohl, A., Binz, H. K., Forrer, P., Stumpp, M. T., Plückthun, A., and

Grütter, M. G. (2003) Designed to be stable: crystal structure of a consensus ankyrin repeat protein. *Proc. Natl. Acad. Sci. U.S.A.* **100,** 1700–1705
41. Eckford, P. D., and Sharom, F. J. (2008) Functional characterization of *Escherichia coli* MsbA: interaction with nucleotides and substrates. *J. Biol. Chem.* **283,** 12840–12850
42. Schultz, K. M., Merten, J. A., and Klug, C. S. (2011) Characterization of the E506Q and H537A dysfunctional mutants in the *E. coli* ABC transporter MsbA. *Biochemistry* **50,** 3599–3608
43. Deleted in proof
44. Jeschke, G., Sajid, M., Schulte, M., and Godt, A. (2009) Three-spin correlations in double electron-electron resonance. *Phys. Chem. Chem. Phys.* **11,** 6580–6591
45. Alvarado, D., Klein, D. E., and Lemmon, M. A. (2010) Structural basis for negative cooperativity in growth factor binding to an EGF receptor. *Cell* **142,** 568–579
46. Renatus, M., Stennicke, H. R., Scott, F. L., Liddington, R. C., and Salvesen, G. S. (2001) Dimer formation drives the activation of the cell death protease caspase 9. *Proc. Natl. Acad. Sci. U.S.A.* **98,** 14250–14255
47. Wiener, M. C. (2004) A pedestrian guide to membrane protein crystallization. *Methods* **34,** 364–372
48. Booth, P. J. (2005) Sane in the membrane: designing systems to modulate membrane proteins. *Curr. Opin. Struct. Biol.* **15,** 435–440
49. Ritchie, T. K., Kwon, H., and Atkins, W. M. (2011) Conformational analysis of human ATP-binding cassette transporter ABCB1 in lipid nanodiscs and inhibition by the antibodies MRK16 and UIC2. *J. Biol. Chem.* **286,** 39489–39496
50. Koide, S. (2009) Engineering of recombinant crystallization chaperones. *Curr. Opin. Struct. Biol.* **19,** 449–457
51. Lee, S. Y., Lee, A., Chen, J., and MacKinnon, R. (2005) Structure of the KvAP voltage-dependent K+ channel and its dependence on the lipid membrane. *Proc. Natl. Acad. Sci. U.S.A.* **102,** 15441–15446